GEOPHYSICAL RESEARCH LETTERS, VOL. 32, L22S10, doi:10.1029/2005GL023732, 2005

Laser pulse reflectance of the ocean surface from the GLAS satellite lidar

Redgie S. Lancaster
Goddard Earth Science and Technology Center, UMBC, Greenbelt, Maryland, USA

James D. Spinhirne
NASA Goddard Space Flight Center, Greenbelt, Maryland, USA

Stephen P. Palm
Science Systems and Applications, Inc., Lanham, Maryland, USA

Received 7 June 2005; revised 29 July 2005; accepted 23 August 2005; published 16 September 2005.

[1] The world's oceans can potentially be used as an extended target for achieving a radiometric calibration of space borne lidar if the reflective properties of the surface can be accurately predicted from available environmental data such as wind speed. To test current understanding of ocean reflectance we compare surface pulse returns measured with the 1064 nm altimetry channel of the Geoscience Laser Altimeter System (GLAS) on the Ice, Cloud and land Elevation Satellite (ICESat) with the predictions of near-IR reflectance from current ocean models. Measurements of wind speed retrieved from the SeaWinds database of the QuikSCAT satellite provide the model input. We find that while ocean models do not provide a full description of the nadir lidar observations this calibration technique yields a precision that exceeds that accomplished using White Sands as a target and that does not require the coordination that accompanies specialized calibration experiments. **Citation:** Lancaster, R. S., J. D. Spinhirne, and S. P. Palm (2005), Laser pulse reflectance of the ocean surface from the GLAS satellite lidar, *Geophys. Res. Lett.*, *32*, L22S10, doi:10.1029/2005GL023732.

1. Introduction

[2] Oceans represent a potentially valuable target for calibrating the measurements of space borne lidar systems. When used in this manner approximately two-thirds of the Earth's surface becomes a calibration source thereby reducing the need for specialized experiments that require the convergence of logistical and environmental conditions. However, the reflective properties of the ocean surface must be accurately predicted from limited environmental data that are readily available on a global basis. The objective of this work is to assess the capability of current ocean reflectance models based upon wind speed to accurately predict the surface return at 1064 nm (hereafter referred to as 1 μm) reported by the Geoscience Laser Altimeter System (GLAS) aboard the Ice, Cloud and land Elevation Satellite (ICESat).

[3] Considerable effort has been directed toward developing an accurate model of ocean reflectance based upon wind speed. The seminal work was conducted by *Cox and Munk* [1954], who reported that the distribution of wave slopes seen in sun-glitter photographs was nearly Gaussian and proposed an empirical relationship between the variance of this distribution (i.e. surface roughness) and wind speed. Subsequently, *Kodis* [1966] showed that ocean reflectance is proportional to the product of the mean number of specular points and their average curvature. *Barrick* [1968] derived expressions for both these quantities based upon the Gaussian surface statistics reported by *Cox and Munk* [1954]. Later *Bufton et al.* [1983] specialized these results to the study of lidar backscatter and investigated experimentally the angular width of the reflectance pattern using an airborne system. *Menzies et al.* [1998] used data from the Lidar In-space Technology Experiment (LITE) instrument to conduct the first study linking orbiting lidar ocean surface reflectance and surface wind speed.

[4] With the launch of the GLAS lidar and its ability to capture the surface pulse return a global set of observations is now available that can be used to evaluate the predictive capabilities of ocean reflectance models. In the paper that follows the model used to predict ocean reflectance is briefly reviewed. Predictions of surface reflectance at a wavelength of 1 μm are then compared with backscatter measurements made in the nadir using the high-speed altimetry channel of GLAS. This paper concludes with a discussion of the utility of using the ocean surface as a remote target of known reflectance and the improvements that need to be made to bring the model predictions into full agreement with the GLAS observations.

2. Ocean Model

[5] At a wavelength of 1 μm ocean reflectance consists predominantly of Fresnel reflection with lesser contributions from scattering by whitecaps and sea foam (hereafter referred to singularly as whitecaps). The reflectance of the ocean surface can be written as

$$R = (1 - W)R_s + WR_f \tag{1}$$

where R_s is the Fresnel reflectance from the surface, R_f is the reflection due to whitecaps and W is the fraction of the surface covered by whitecaps. Following the development

0094-8276/05/2005GL023732$05.00

Table 1. Clear-Air Data Segments Used in the Current Work Along With the Corrective Scaling Terms Employed to Compensate for Changes in the Boresite

Date	Track	Segment (Lat, Elon)$_i$	Segment (Lat, Elon)$_f$	Asc. Node LT (hh:mm)	Desc. Node LT (hh:mm)	Boresite Scale Factor
				Laser 1		
Feb 21	77	−50.6, 302.9	−45.2, 301.7	04:37	16:37	1
Feb 25	20	20.9, 69.2	16.9, 68.6	04:29	16:29	1
Feb 25	25	−43.1, 298.7	−52.9, 296.5	04:29	16:29	1
Mar 4	10	−41.7, 302.0	−48.9, 300.5	04:16	16:16	1
Mar 5	18	20.9, 69.2	16.9, 68.6	04:15	16:15	1
Mar 19	113	−56.9, 153.4	−52.1, 152.1	03:49	16:49	1
				Laser 2a		
Oct 5	1111	−35.9, 306.1	−50.9, 303.1	21:42	09:42	1.828
Oct 8	1156	5.1, 134.0	21.9, 131.7	21:36	09:36	2.039
Oct 9	1171	−34.9, 112.7	−10.1, 109.0	21:34	09:34	2.039
Oct 16	1283	23.6, 298.7	33.9, 297.0	21:21	09:21	1.359
Oct 26	77	−53.0, 305.8	−40.1,303.0	21:03	09:03	1.359
Nov 3	196	−44.9, 304.7	−40.1, 303.8	20:48	08:48	1.293

of *Bufton et al.* [1983] the Fresnel reflectance (R_s) is described by

$$R_s \equiv \rho_{eff} = \rho \frac{\Omega_L}{\Omega} = \frac{\rho}{4\langle S^2 \rangle} \qquad (2)$$

where ρ is the Fresnel reflection coefficient, Ω is the solid angle of the backscatter pattern, ρ_{eff} is the reflection coefficient of an equivalent Lambertian reflector, and Ω_L is the solid angle (π/cos θ) of the Lambertian pattern. At nadir ($\theta = 0$, $\Omega_L = \pi$) the ocean backscatter solid angle can be written as $\Omega = 4\pi\langle S^2\rangle$ where $\langle S^2\rangle$ is the variance of the distribution of wave slopes. The Fresnel reflection coefficient, $\rho = 0.02$, is computed from the tabulations of *Hale and Querry* [1973]. *Cox and Munk* [1954] provide an empirical description of $\langle S^2\rangle$ as a function of wind speed

$$\langle S^2 \rangle = 0.003 + 5.12 \times 10^{-3} U_{12.4} \qquad (3)$$

where $U_{12.4}$ is the wind speed at 12.4 m above the ocean surface. *Bufton et al.* [1983] and *Menzies et al.* [1998] alternatively employ a relation by *Wu* [1972]

$$\langle S^2 \rangle = \begin{cases} (\ln U_{10} + 1.2) \times 10^{-2} & U_{10} \le 7\,\mathrm{m/s} \\ (0.85 \ln U_{10} - 1.45) \times 10^{-1} & U_{10} > 7\,\mathrm{m/s} \end{cases} \qquad (4)$$

derived from a reanalysis of the *Cox and Munk* [1954] data.

[6] In computing the ocean lidar return from whitecaps the relative area of the ocean surface that they cover is estimated from the relation

$$W = [2.95 \pm 6.1] \times 10^{-6}\, U_{10}^{3.52 \pm 0.52} \qquad (5)$$

reported by *Monahan and O'Muircheartaigh* [1980]. The stated uncertainties in the above coefficients have been added as part of the current work and are computed from the results of the different authors included in the *Monahan and O'Muircheartaigh* [1980] survey. The current work uses $R_f = 0.2$ [*Koepke*, 1984] as the Lambertian reflectance of typical oceanic whitecaps at a wavelength of 1 μm.

3. Data

[7] The current work compares retrievals of ocean surface reflectance reported in the ICESat GLA05 L1B Waveform-based Range Correction Data with the values predicted by equation (1). The reported reflectance parameter (*i_reflctUncorr*) represents the area under the return pulse and is not corrected for atmospheric attenuation. To minimize the systematic errors that arise from an incomplete knowledge of the atmospheric attenuation a survey of the GLAS data was conducted to identify segments that are free of clouds and that exhibit low amounts of aerosol scattering. A listing of the dates, tracks and geographic coordinates of the data segments that were selected is shown in Table 1. In all cases GLAS was pointing approximately 0.1 degrees off-nadir (hereafter treated as nadir). The estimates of wind speed required in equations (3)–(5) of the ocean reflectance model were obtained from the SeaWinds scatterometer database of the QuikSCAT satellite.

[8] The SeaWinds and GLAS measurements are not coincident. QuikSCAT is in a sun-synchronous orbit with a nominal local equator crossing time at the ascending node of 0600 whereas the corresponding time of the ICESat ascending node migrates westward by approximately 0.5 degrees each day. It is seen in the data of Table 1 that the equator crossing time of GLAS migrates from 0437 to 0349 LT during the first of two included observation periods and from 2142 to 2048 LT in the second. The spatial resolution offered by the two instruments also differs with SeaWinds measurements being available on a 25 km grid and GLAS offering a spatial resolution of 70 m with 170 m along-track spacing. To compare the data products of these two instruments the GLAS results were binned into 1-second intervals (40 pulse returns) and registered with the nearest SeaWinds observations. All GLAS 1-second averages registered to a common element on the SeaWinds grid were also averaged.

[9] The results presented here are those derived from GLAS measurements made during the Laser 1 and Laser 2a observing periods of 2003 and are reported in Releases 18 and 19 of the ICESat data products, respectively. Two adjustments related to attenuation, that include a correction of the Laser 2a data to compensate for changes in the boresite and a correction of both the Laser 1 and Laser 2a data for atmospheric attenuation, have been applied to the retrieved data product. The corrections used in the boresite adjustment are shown in Table 1 and were gleaned from a comparison of 1 μm and 532 nm returns from cirrus clouds coupled with coincident ER-2 underflight measurements.

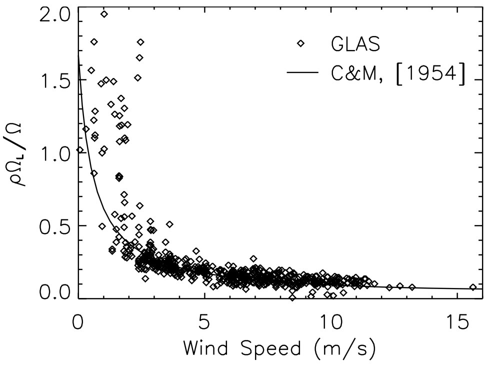

Figure 1. Reported and modeled ocean reflectance for the nadir GLAS observations of Table 1. The model predictions use the *Cox and Munk* [1954] (equation (3)) model of ocean surface statistics.

The corrections used to compensate for atmospheric attenuation were computed from the sum of the molecular and aerosol optical depths reported in the GLA11 data product (more recent data releases incorporate this latter correction) [*Spinhirne et al.*, 2005]. There are no optical depths reported in the GLA11 database for Laser 1 observations so the average optical depth of 0.05 ± 0.04 identified for the selected Laser 2a cases is used instead.

[10] Shown in Figure 1 is a comparison of reported and modeled (using the *Cox and Munk* [1954] relation of equation (3)) ocean reflectance for the GLAS observations. The model predictions of Figure 1 compare favorably with GLAS observations logged at wind speeds greater than 3 m/s. For winds less than about 3 m/s the reported reflectance tends to exceed the model predictions and the scatter in the data increases. One candidate cause of this scatter at low wind speeds is the SeaWinds measurement precision.

[11] According to the QuikSCAT mission requirement SeaWinds can measure winds ranging from 3 to 20 m/s with a 2 m/s standard deviation. A comparison of SeaWinds scatterometer measurements with those of TOPEX and ERS-2 altimeters by *Queffeulou and Bentamy* [2000] confirms this performance indicating a standard deviation of 0.7 m/s at "low winds," 1 m/s at 10 m/s and 2.2 m/s at 20 m/s. For winds greater than about 3 m/s an error of 1–2 m/s in the speed assignment represents minor differences in the comparison between reported and modeled reflectance. Below 3 m/s a scatter of 0.7 m/s in the wind assignment encompasses a large range of reflectance predictions.

[12] *Jelenak et al.* [2002] additionally find evidence from a comparison with in-situ buoy measurements that SeaWinds overestimates winds less than about 3 m/s by 1 to 2 m/s. The effect of such a bias on the current work is an apparent inflation of the reflectance measurements at the lowest winds as they are logged at greater speeds for which the model predicts less reflectance. This suggests that there is an upper limit on the near-IR surface reflectance for which a comparison with model predictions based upon SeaWinds measurements can be expected to be valid, which is taken to be R = 1.0 in the current work. Figure 2 shows the subset of surface observations having an equivalent Lambertian reflectance less than this amount binned into 0.5 m/s averages. Model predictions based upon both the *Cox and Munk* [1954] relation of equation (3) and the *Wu* [1972] relation of equation (4) are included in Figure 2 for comparison as is the contribution due to whitecaps.

[13] For the subset of observations shown in Figure 2 the model predictions based upon the *Cox and Munk* [1954] surface statistics are in good agreement with measurements logged at wind speeds of 1–6 m/s as reported by SeaWinds. However, this same model underestimates ocean reflectance in the regime of 6 to 12 m/s with an oscillation apparent in the measurements that is not reproduced by the predictions. Measurements of reflectance for winds greater than 12 m/s are difficult to find in data segments free of clouds but the model appears to predict with reasonable agreement those few that are located. By contrast the model predictions based upon the surface statistics of *Wu* [1972] underestimate the measurements for wind speeds between 1 and 5 m/s as logged by the SeaWinds scatterometer. Apart from a discontinuity at 7 m/s they tend to be in better agreement with measurements at speeds between 5 and 10 m/s. For winds greater than 10 m/s the two models of surface statistics are in agreement with one another. The contribution of whitecaps to the nadir lidar measurements is seen in Figure 2 to be negligible.

[14] The observations of Lambertian surface reflectance greater than R = 1.0 that are excluded from the comparison of Figure 2 are not random occurrences governed by outlier statistics. Rather, these correspond to areas that exhibit a particularly calm ocean surface which cover a limited spatial extent. This is seen in Figure 3 where the measured reflectance from four data segments is plotted as a function of latitude showing a full-width at half maximum of 2 to 4 degrees. The upper limit of surface reflectance predicted by the model using the *Cox and Munk* [1954] relation of equation (3) is $R_{max} = 1.7$ and is exceeded in all four cases. Thus, while these ocean model predictions are seen in Figure 2 to be in agreement with measurements for wind speeds as low as 1 m/s they appear to underestimate the reflectance for surfaces governed by lesser winds. The *Wu* [1972] model predictions approach infinity at U = 0.3 m/s.

4. Discussion and Conclusions

[15] A coordinated experiment that included a calibration of the local surface reflectance against a standard target

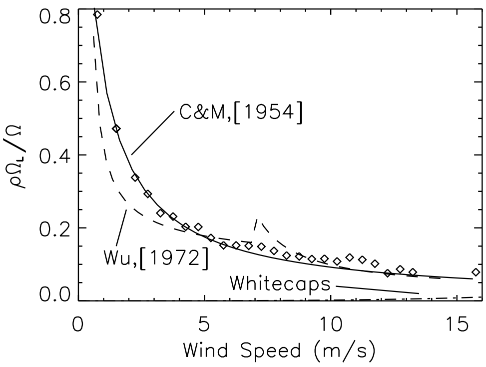

Figure 2. Predictions of ocean surface reflectance using equations (3) and (4) separately are compared with surface returns reported by GLAS. The measurements have been binned into 0.5 m/s intervals and only those with an equivalent Lambertian reflectance less than 1.0 are included in the average. Also shown is the reflectance due to whitecaps.

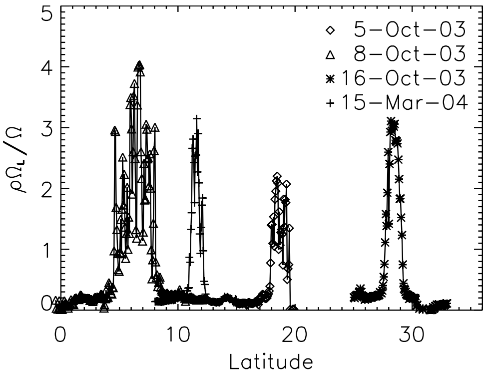

Figure 3. Reported reflectance from four GLAS data segments that exhibit particularly calm ocean surface.

[*Biggar et al.*, 2003] and simultaneous measurements of atmospheric transmission was conducted at the White Sands missile test range in March 2003 as part of the ICESat operations in an effort to characterize the GLAS surface pulse return. The ratio of the GLAS and ground-based measurements of surface pulse reflectance was found to be 1.12 ± 0.10. For comparison a ratio of 1.08 ± 0.05 is found for the measured and predicted ocean reflectance using the data of Figure 2. This 8 percent bias between measurement and model is within the stated precision of the White Sands calibration and the 5 percent standard deviation is more precise than that achieved during the coordinated experiment.

[16] The effects of saturation complicated interpretation of the White Sands data. The response of the GLAS 1 μm channel receiver departs from linearity when the collected backscattered energy exceeds 8 fJ, which corresponds to a Lambertian reflectance of about 0.5 for the 67 mJ pulse energy of that period. As can be seen by inspection of Figure 1 this saturation does not affect the majority of ocean measurements as they exhibit a reflectance less than about 0.4. In addition, logistical difficulties resulted in the White Sands surface calibration being performed several days after the GLAS observations. By contrast the time differential between GLAS and Seawinds was less than 4 hours. Hence, GLAS observations of ocean reflectance made under differing surface conditions can provide end-to-end calibrations that are both more regular and more precise than that accomplished using White Sands as a target.

[17] The accuracy of a calibration based upon measurements of ocean reflectance depends upon the model of surface statistics that is employed. Of the two models included in this work it is *Cox and Munk*'s [1954] model that provides the better overall agreement. However, it appears that a more complex model of surface statistics is required to properly account for the features likely due to the influence of capillary and capillary-gravity waves seen at greater wind speeds. For the purpose of calibration it is not necessary to model these effects or those of whitecaps (which are seen to be negligible in the current work) from first principles but rather an empirically determined model should suffice. While doing so is beyond the immediate scope of the current work the extensive global dataset of GLAS provides sufficient statistics from which this model can be determined.

[18] Finally, the SeaWinds instrument is not ideal for logging observations of ocean reflectance for those surfaces driven by winds less than 3 m/s as this speed represents the lower limit of its adopted operating range. Hence, the present survey would benefit from a second source of wind measurements that are more sensitive to low wind speeds such as those from the NOAA network of ocean buoys. Still, the agreement in this regime between the predictions using the *Cox and Munk* [1954] model of surface statistics and those measurements having an equivalent Lambertian reflectance less than 1.0 is intriguing as it implies that the uncertainties accompanying the SeaWinds measurements below 3 m/s actually originate in measurements of surfaces driven by winds less than 1 m/s. The addition of a surface lidar to future operational wind missions could be used to discriminate between these cases and extend the operating range of the microwave wind measurements.

[19] **Acknowledgment.** We thank NASA's ICESat Science Project and the NSIDC for distribution of the ICESat data, see http://icesat.gsfc.nasa.gov and http://nsidc.org/data/icesat/.

References

Barrick, D. E. (1968), Rough surface scattering based on the specular point theory, *IEEE Trans. Antennas Propag.*, *14*, 449–454.

Biggar, S. F., K. J. Thome, and W. Wisniewski (2003), Vicarious radiometric calibration of EO-1 sensors by reference to high-reflectance ground targets, *IEEE Trans. Geosci. Remote Sens.*, *41*, 1174–1179.

Bufton, J. L., F. E. Hoge, and R. N. Swift (1983), Airborne measurements of laser backscatter from the ocean surface, *Appl. Opt.*, *22*, 2603–2618.

Cox, C., and W. Munk (1954), Measurement of the roughness of the sea surface from photographs of the Sun's glitter, *J. Opt. Soc. Am.*, *44*, 838–850.

Hale, G. M., and M. E. Querry (1973), Optical constants of water in 200-nm to 200-μm wavelength region, *Appl. Opt.*, *12*, 555–563.

Jelenak, Z., L. N. Connor, and P. S. Chang (2002), The accuracy of high resolution winds from QuikSCAT, in *IGARSS 2002: Remote Sensing, Integrating Our View of the Planet: 2002 IEEE International Geoscience and Remote Sensing Symposium*, vol. 2, pp. 732–734, Inst. of Electr. and Electr. Eng., New York.

Kodis, R. D. (1966), A note on the theory of scattering from an irregular surface, *IEEE Trans. Antennas. Propag.*, *14*, 77–82.

Koepke, P. (1984), Effective reflectance of oceanic whitecaps, *Appl. Opt.*, *23*, 1816–1824.

Menzies, R. T., D. M. Tratt, and W. H. Hunt (1998), Lidar in-space technology experiment measurements of sea surface directional reflectance and the link to surface wind speed, *Appl. Opt.*, *37*, 5550–5559.

Monahan, E. C., and I. O'Muircheartaigh (1980), Optimal power-law description of oceanic whitecap coverage dependence on wind speed, *J. Phys. Oceanogr.*, *10*, 2094–2099.

Queffeulou, P., and A. Bentamy (2000), Comparison between QuikSCAT and altimeter wind speed measurements, in *IGARSS 2000: IEEE 2000 International Geoscience and Remote Sensing Symposium: Taking the Pulse of the Planet, the Role of Remote Sensing in Managing the Environment*, vol. 2, edited by T. I. Stein, pp. 269–271, Inst. of Electr. and Electr. Eng., New York.

Spinhirne, J. D., S. P. Palm, W. D. Hart, D. L. Hlavka, and E. J. Welton (2005), Cloud and aerosol measurements from GLAS: Overview and initial results, *Geophys. Res. Lett.*, doi:10.1029/2005GL023507, in press.

Wu, J. (1972), Sea-surface slope and equilibrium wind-wave spectra, *Phys. Fluids*, *13*, 741–747.

R. S. Lancaster, Goddard Earth Science and Technology Center, UMBC, Code 613.1, Greenbelt, MD 20771, USA. (lancaster@virl.gsfc.nasa.gov)

S. P. Palm, Science Systems and Applications Inc., Lanham, MD 20706, USA.

J. D. Spinhirne, Laboratory for Atmospheres, Code 613.1, NASA Goddard Space Flight Center, Greenbelt, MD 20771, USA.